Selective Optical Property Modification of Double-Walled Carbon Nanotubes by Fluorination

Takuya Hayashi,[†],* Daisuke Shimamoto,[†] Yoong Ahm Kim,[†] Hiroyuki Muramatsu,[†] Fujio Okino,[‡] Hidekazu Touhara,[‡] Takashi Shimada,[§] Yuhei Miyauchi,[§] Shigeo Maruyama,[§] Mauricio Terrones,[⊥] Mildred S. Dresselhaus,[‖] and Morinobu Endo[†]

[†]Faculty of Engineering, Shinshu University, 4-17-1 Wakasato, Nagano-shi 380-8553, Japan, [‡]Faculty of Textile Science and Technology, Shinshu University, 3-15-1 Tokida, Ueda 386-8567, Japan, [§]Department of Mechanical Engineering, The University of Tokyo, 7-3-1 Hongo, Bunkyo-ku, Tokyo 133-8656, Japan, [⊥]Advanced Materials Department, IPICYT, Camino a la Presa San José 2055, Col. Lomas 4. Sección, San Luis Potosí 78216, México, and [‖]Massachusetts Institute of Technology, Cambridge, Massachusetts 02139-4307

ABSTRACT We found that by fluorination of double-walled carbon nanotubes (DWNTs), it is possible to suppress only the Raman radial breathing mode and absorption peaks from the outer (large diameter) tubes of DWNTs. In contrast, Raman signals from the inner shells showed no difference from the pristine DWNTs. The stability of the inner shells of fluorinated DWNTs was also confirmed from the photoluminescence (PL) map and the optical absorption spectra, which only showed the signals from the inner shells of DWNTs, with no distinct change in the optical properties of the inner tubes after fluorination. Our results indicate that once fluorinated, there exists only a weak, if not none, interaction between the inner tube and the outer fluorinated tube, proving that fluorination can be used to suppress the optical properties of carbon nanotubes without interfering the properties of inner tubes. The present finding can be important in electronic and sensor applications, keeping the inner tube from having unwanted contact with other substances that may distract from the inner tube's own characteristics.

KEYWORDS: double-walled carbon nanotube · fluorination · photoluminescence

Fluorination is known to be an useful method to modify the surface properties of conventional carbons,[1,2] and therefore intensive studies related to the fluorination of single-walled and multi-walled carbon nanotubes (SWNTs and MWNTs, respectively) have been carried out from the theoretical[3–5] and experimental[6–8] standpoints, not only for tailoring the electronic states of the tubes but also to improve the dispersability of carbon nanotubes. Recently, mildly fluorinated SWNTs and their subsequent thermal treatment were demonstrated to be efficient to remove metallic SWNTs.[9] The systematic structural characterizations on heavily fluorinated MWNTs also revealed[10] that there is some reversibility in the fluorination process; that is, fluorine atoms can detach from the carbon network during the heat-treatment process without damaging the carbon network. Moreover, it became clear that depending on the fluorination level, fluorine incorporated into carbon nanotubes has different bonding states known as ionic and covalent bonding.

More recently, nanotube researchers have paid much attention to double-walled carbon nanotubes (DWNTs) because these coaxial tubules were shown to exhibit higher structural and emitting stability when compared to SWNTs.[11,12] In addition, a DWNT (the simplest MWNT) has been utilized as an ideal theoretical model for studying the interaction and coupling behaviors between concentric tubes.[13–16] Unfortunately, there is no experimental evidence for understanding intertube interactions, because it is not possible to produce pure samples of DWNTs (with 100% purity and the total absence of SWNTs) using presently available synthesis techniques. Even though some photoluminescence (PL) studies have been reported for catalytically grown DWNTs containing small fractions of SWNTs[17] and high purity of DWNTs (~90%) using the selective removal of SWNTs *via* oxidation treatments,[18] it is not easy to completely discard the effects of SWNTs as impurity.

In this study, we prepared high-purity DWNT-derived buckypaper (>95%) by combining the catalytic chemical vapor deposition method and a subsequent oxidation process.[19] Fluorination of the DWNT buckypaper was performed using a furnace with DWNT buckypaper under fluorine gas flow, as detailed in other literature.[20] For these fluorinated DWNTs, we carried out systematic optical studies, including PL, optical absorption and resonant Raman scattering,
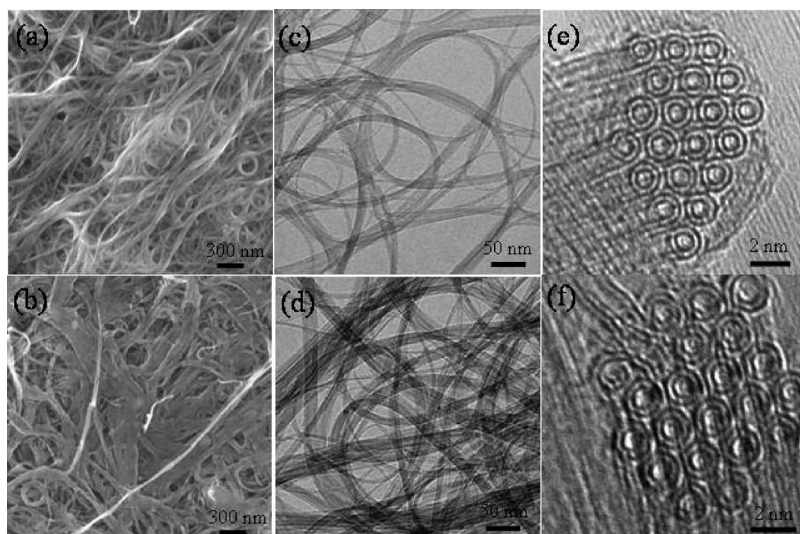
Figure 1. FE-SEM and TEM images of pristine (a, c, and e) and fluorinated (b, d, and f) DWNTs, respectively.
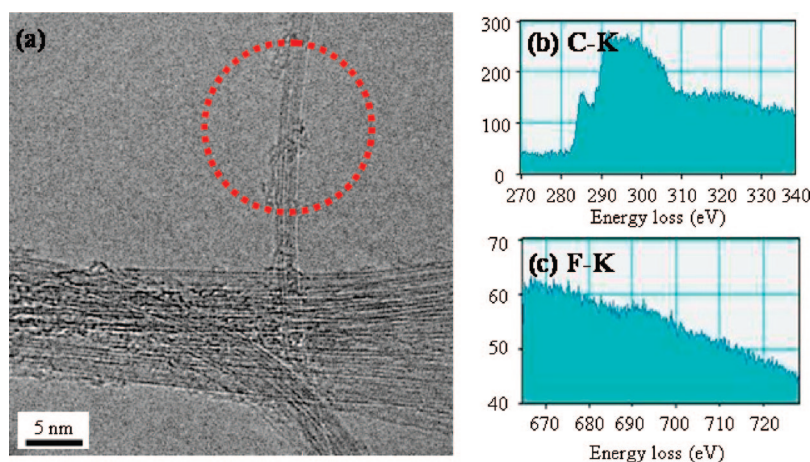

Figure 2. (a) TEM image of a single fluorinated DWNT and its corresponding electron energy loss spectra for (b) C−K and (c) F−K edges.
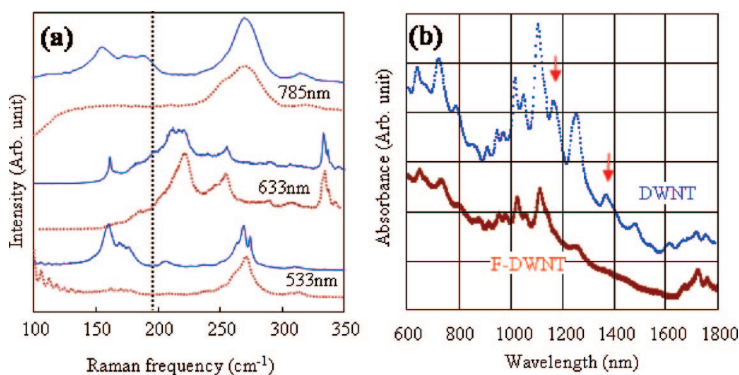

Figure 3. (a) Low-frequency Raman spectra of pristine and fluorinated DWNTs using three different laser lines (532, 633, and 785 nm). (b) UV absorption spectra of the pristine and fluorinated DWNTs. The solid and dotted lines indicate the pristine and fluorinated DWNTs, respectively.

and transmission electron microscopy/electron energy losss spectroscopy (TEM/EELS) observations. Our results demonstrate that the PL map and absorption peaks only arise from the inner tubes of the fluorinated DWNTs, because the fluorinated outer DWNTs and remains of SWNTs became optically inactive.

RESULTS AND DISCUSSION

Field emission scanning electron microscopy (FE-SEM) and TEM images of pristine and fluorinated DWNT are shown in Figure 1. The FE-SEM image (Figure 1 b) depicts the rather brittle nature of the fluorinated sample exhibiting less tube flexibility. However, from the TEM images, there was no clear change in the bundle structure including the coaxial morphology, and the fact that the tubes were fluorinated was not clear. However, from the EELS analysis from single fluorinated DWNT, we managed to detect the hump-like signal corresponding to the ionization K-edge of fluorine (located at ∼690 eV) (see Figure 2c).

Although we were able to confirm that the DWNT sample was indeed fluorinated, it was not clear whether all the layers were fluorinated or not. In such a case, information obtained from the Raman radial breathing mode (RBM) is effective because if a tube is fluorinated, the RBM corresponding to that tube disappears due to the structural change and/or the change of the resonant energies experienced in the graphene network of a nanotube. Figure 3a shows the low-frequency Raman spectra for both pristine and fluorinated DWNTs, respectively. We have acquired the Raman spectra with three different laser lines: 532, 633, and 785 nm. We noted that the Raman D-band (defect induced mode)[21,22] was not observed for the pristine sample but became clear after fluorination (not shown here), which suggests that a certain amount of disorder was introduced into the graphene network of carbon nanotubes due to the interaction of F atoms with the outer nanotube surface. These interactions suppress the RBM because it is difficult to maintain a perfect cylindrical shape after F atoms are covalently bonded to the carbon atoms of the nanotube. In particular, in the RBM signal region, a lower frequency (<200 cm^{-1}) feature originating from the outer tube was not found after fluorination, whereas the RBM from the inner tube (located at higher RBM frequencies) remains almost unchanged. Furthermore, it is expected that when a nanotube is fluorinated, the band gap of nanotubes becomes larger than
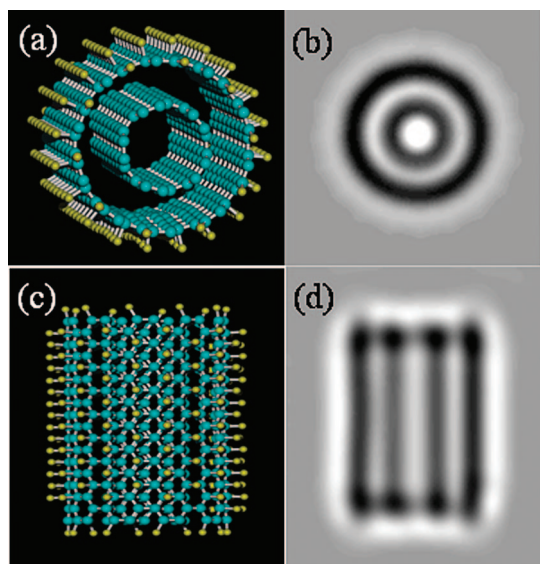
Figure 4. Cross-sectional (a) and longitudinal (c) models of the fully fluorinated outer shell of the DWNT and their corresponded simulated images (b, d), respectively.

the energy of Raman probe laser so that the resonant Raman signal should disappear. This again suggests that fluorination has occurred selectively only at the outer tube of DWNTs and the inner tube remained unaffected. In order to support the selective attachment of fluorine atoms on the outer tubes of the DWNT, we measured the UV–vis–NIR absorption spectra from individualized nanotube solutions (see Figure 3b). In this case, sharp absorption multipeaks provide strong evidence for individual carbon nanotubes in D_2O. It is noteworthy that the selective depression of absorption peaks at 1180 and 1375 nm is closely related to the fluorinated outer tubes because this region is overlapped by the E^S_{22} of the outer tubes and the E^S_{11} of the inner tubes. Here again, we proved that fluorine atoms react with the outer shell preferentially and leave the inner tubes intact. In addition, TEM image simulation of the models with selectively and symmetrically fluorinated outer shells of the DWNT (Figure 4) showed that no big difference is found when compared with the TEM image of pristine DWNT, which was the case with the actual TEM observation.

Similar phenomena were found in the PL map (Figure 5). Due to the limitation of the instrument, we were only able to capture the information from the inner tubes of the DWNTs. From the pristine sample (Figure 5a), three strong PL peaks were ascribed to the inner tubes with chiralities (8,4), (7,6), and

(7,5). After fluorination (Figure 5b), we observed the strongest PL intensity corresponding to (7,5) tubes and the disappearance of signals assigned to relatively small sized tubes exhibiting diameters of *ca.* 0.7–0.8 nm. There are some possible reasons for the present change in the relative PL intensities: Fluorine atoms have reacted with the SWNTs that survived the purification process, small diameter DWNTs with higher chemical activity have decomposed, or the selectivity in the dispersion process has changed by fluorination. However, since fluorinated SWNTs become optically inactive, the measured PL map can be considered to be arising from the inner tubes of the DWNTs and not from the SWNT. Hence we can safely conclude that the inner tubes of DWNTs are visible in PL and the electronic structure is not disturbed by the outer tube.

In the present study, we have shown that in the fluorination process of DWNTs mainly the outer tube is fluorinated and the inner tube remains almost unaffected by fluorine atoms. When compared to SWNTs synthesized with the chemical vapor deposition process, the inner tube of a DWNT has a smaller diameter distribution due to the confinement and interaction with the outer tube that limits the diameter of the inner tube. As demonstrated in the present study, by choosing the proper fluorination conditions, it is possible to passivate the outer tube, leaving the inner tube optically active. PL and Raman studies demonstrated that screening effects of the inner tube chirality have effectively taken place during the fluorination process. The passivated outer tube can act as a nanosheath that prevents the inner tube from interacting with other tubes, which can be effective for producing CNT-based integrated circuits, where overlapping of CNTs is inevitable.
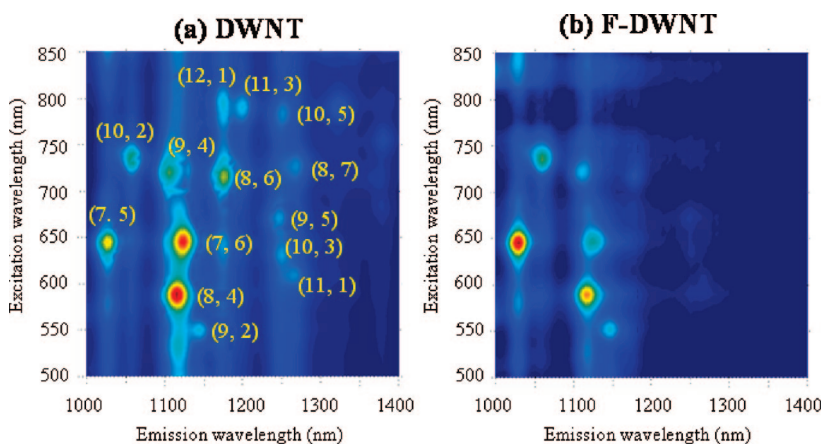

Figure 5. Photoluminescence map for the pristine (a) and fluorinated (b) DWNTs, respectively.

METHODS

The synthesized high-purity DWNT-derived buckypaper[19] was thermally treated at 1200 °C in argon to remove the poten-

tially incorporated SWNTs. Fluorination of the purified DWNT was performed by passing fluorine gas (1 atm) at 200 °C for 5 h and the stoichiometry of the fluorinated DWNTs corresponded

to $CF_{0.3}$.[20] Structural characterization of fluorinated DWNTs was carried out by Raman spectroscopy (Kaiser Hololab, 532, 633, and 785 nm), FE-SEM (JEOL JSM-6335F), and TEM (JEOL JEM 2010FEF and 2100F). In order to obtain well-defined PL map and absorption peaks,[23–25] we prepared homogeneously dispersed nanotube suspensions as follows:[26,27] 1 mg of pristine and fluorinated DWNTs were dispersed in D_2O (10 g) with 50 mg of sodium dodecylbenzene sulfonate (NaDDBS) under a strong sonication ($\sim$470 W/cm^2) for 1 h at 4 °C. Subsequently, we subjected these suspensions (containing carbon nanotubes) to an ultracentrifuge (489000g) and finally obtained well-dispersed individual DWNTs (pristine and fluorinated).

REFERENCES AND NOTES

1. Nakajima, T. Fluorine-Carbon and Fluoride-Carbon Materials: Chemistry, Physics, and Applications; CRC: Boca Raton, FL, 1994.
2. Touhara, H.; Okino, F. Property Control of Carbon Materials by Fluorination. *Carbon* **2000**, *38*, 241–267.
3. Kudin, K. N.; Bettinger, H. F.; Scuseria, G. E. Fluorinated Single-Wall Carbon Nanotubes. *Phys. Rev. B* **2001**, *63*, 045413.
4. Park, K. A.; Choi, Y. S.; Lee, Y. H. Atomic and Electronic Structures of Fluorinated Single-Walled Carbon Nanotubes. *Phys. Rev. B* **2003**, *68*, 045429.
5. Zhao, J.; Park, H.; Han, J.; Lu, J. P. Electronic Properties of Carbon Nanotubes with Covalent Sidewall Functionalization. *J. Phys. Chem. B* **2004**, *108*, 4227–4230.
6. Mickelson, E. T.; Huffman, C. B.; Rinzler, A. G.; Smalley, R. E.; Hauge, R. H.; Margrave, J. L. Fluorination of Single-Wall Carbon Nanotubes. *Chem. Phys. Lett.* **1998**, *296*, 188–194.
7. An, K. H.; Heo, J. G.; Jeon, K. G.; Bae, D. J.; Jo, C.; Yang, C. W.; Park, C. Y.; Lee, Y. H.; Lee, Y. S.; Chung, Y. S. X-ray Photoemission Spectroscopy Study of Fluorinated Single-Walled Carbon Nanotubes. *Appl. Phys. Lett.* **2002**, *80*, 4235–4238.
8. Kawasaki, S.; Komatsu, K.; Okino, F.; Tohara, H.; Kataura, H. Fluorination of Open- and Closed-end Single-Walled Carbon Nanotubes. *Phys. Chem. Chem. Phys.* **2004**, *6*, 1769–1772.
9. Yang, C. M.; An, K. H.; Park, J. S.; Park, K. A.; Lim, S. C.; Cho, S. H.; Lee, Y. S.; Park, W. J.; Park, C. Y.; Lee, Y. H. Preferential Etching of Metallic Single-Walled Carbon Nanotubes with Small Diameter by Fluorine Gas. *Phys. Rev. B* **2006**, *73*, 075419.
10. Hayashi, T.; Terrones, M.; Scheu, C.; Kim, Y. A.; Ruhle, M.; Nakajima, T.; Endo, M. NanoTeflons: Structure and EELS Characterization of Fluorinated Carbon Nanotubes and Nanofibers. *Nano Lett.* **2002**, *2*, 491–496.
11. Kurachi, H.; Uemura, S.; Yotani, J.; Nagasako, T.; Yamada, H.; Ezaki, H.; Maesoba, T.; Loutfy, R.; Moravsky, A.; Nakazawa, T.; Saito, Y. FED with Double-Walled Carbon Nanotube Emitters. *Proceedings of 21st International Display Research Conference/8th International Display Workshops*; Society for Information Display: San Jose, CA, 2001; pp 1237–1240.
12. Kim, Y. A.; Muramatsu, H.; Hayashi, T.; Endo, M.; Terrones, M.; Dresselhaus, M. S. Thermal Stability and Structural Changes of Double-Walled Carbon Nanotubes by Heat Treatment. *Chem. Phys. Lett.* **2004**, *398*, 87–92.
13. Saito, R.; Matsuo, R.; Kimura, T.; Dresselhaus, G.; Dresselhaus, M. S. Anomalous Potential Barrier of Double-Wall Carbon Nanotube. *Chem. Phys. Lett.* **2001**, *348*, 187–193.
14. Chen, J.; Yang, L.; Yang, H.; Dong, J. Electron Transport Properties of Incommensurate Double-Walled Carbon Nanotubes. *Chem. Phys. Lett.* **2004**, *400*, 384–388.
15. Liang, S.-D. Intrinsic Properties of Electronic Structure in Commensurate Double-Wall Carbon Nanotubes. *Physica B* **2004**, *352*, 305–311.
16. Song, W.; Ni, M.; Lu, J.; Gao, Z.; Nagase, S.; Yu, D.; Ye, H.; Zhang, X. Electronic Structures of Semiconducting Double-Walled Carbon Nanotubes: Important Effect of Interlayer Interaction. Fluorescence Spectroscopy of Single-Walled Carbon Nanotubes Synthesized From Alcohol. *Chem. Phys. Lett.* **2005**, *414*, 429–433.
17. Hertel, T.; Hagen, A.; Talaaev, V.; Arnold, K.; Hennrich, F.; Kappes, M.; Rosenthal, S.; McBride, J.; Ulbricht, H.; Flahaut, E. Spectroscopy of Single- and Double-Wall Carbon Nanotubes in Different Environments. *Nano Lett.* **2005**, *5*, 511–514.
18. Kishi, N.; Kikuchi, S.; Ramesh, P.; Sugai, T.; Watanabe, Y.; Shinohara, H. Enhanced Photoluminescence From Very Thin Double-Wall Carbon Nanotubes Synthesized by The Zeolite-CCVD Method. *J. Phys. Chem. B* **2006**, *110*, 24816–24821.
19. Endo, M.; Muramatsu, M.; Hayashi, T.; Kim, Y. A.; Terrones, M.; Dresselhaus, M. S. 'Buckypaper' From Coaxial Nanotubes. *Nature* **2005**, *433*, 476.
20. Muramatsu, M.; Kim, Y. A.; Hayashi, T.; Endo, M.; Yonemoto, A.; Arikai, H.; Okino, F.; Touhara, H. Fluorination of Double-Walled Carbon Nanotubes. *Chem. Commun.* **2005**, 2002–2004.
21. Thomsen, C.; Reich, S. Double Resonant Raman Scattering in Graphite. *Phys. Rev. Lett.* **2000**, *85*, 5214–5217.
22. Saito, R.; Jorio, A. G.; Souza Filho, A.; Dresselhaus, G.; Dresselhaus, M. S.; Pimenta, M. A. Probing Phonon Dispersion Relations of Graphite by Double Resonance Raman Scattering. *Phys. Rev. Lett.* **2002**, *88*, 027401.
23. O'Connell, M. J.; Bachilo, S. M.; Huffman, C. B.; Moore, V. C.; Strano, M. S.; Haroz, E. H.; Rialon, K. L.; Boul, P. J.; Noon, W. H.; Kittrell, C.; Ma, J.; Hauge, R. H.; Weisman, R. B;. Smalley, R. E. Band Gap Fluorescence From Individual Single-Walled Carbon Nanotubes. *Science* **2002**, *297*, 593–596.
24. Bachilo, S. M.; Strano, M. S.; Kittrell, C.; Hauge, R. H.; Smalley, R. E.; Weisman, R. B. Structure-Assigned Optical Spectra of Single-Walled Carbon Nanotubes. *Science* **2002**, *298*, 2361–2366.
25. Miyauchi, Y.; Chiashi, S.; Murakami, Y.; Hayashida, Y.; Maruyama, S. Fluorescence Spectroscopy of Single-Walled Carbon Nanotubes Synthesized From Alcohol. *Chem. Phys. Lett.* **2004**, *387*, 198–203.
26. Miyauchi, Y.; Maruyama, S. Identification of An Excitonic Phonon Sideband by Photoluminescence Spectroscopy of Single-Walled Carbon-13 Nanotube. *Phys. Rev. B* **2006**, *74*, 35415.
27. Miyauchi, Y.; Oba, M.; Maruyama, S. Cross-polarized Optical Absorption of Single-Walled Nanotubes by Polarized Photoluminescence Excitation Spectroscopy. *Phys. Rev. B* **2006**, *74*, 205440.